THE SULFUR EFFECT ON THE MICROSTRUCTURE AND MECHANICAL PROPERTIES OF THE ABNT 1045 STEEL

Diego Fernando Gonzalez Santos, diego_gsim@yahoo.com.mx
Eduardo Bugelli, eduardo.bugelli@poli.usp.br
Larissa Driemeier, driemeie@usp.br
Izabel Fernanda Machado, machadoi@usp.br
Departamento de Engenharia Mecatrônica e Sistemas Mecânicos. Escola Politécnica da Universidade de São Paulo.
Av. Prof. Mello Moraes, 2231. 05508-900 Sao Paulo, S.P. Brazil

Abstract. *The mechanical properties can be described as the relationship between the stress and the resistance of the material to deformation and fracture. However, the response of the material to stress is significant different at low and high strain rates. Therefore, there are several tests to measure the mechanical properties, wherein the loading and the strain rates are different to evaluate the features of the material. This work deals with the sulfur influence on the microstructure and on the static and dynamic behavior of two steels with similar chemical composition (ABNT 1045). Microstructural characterization of the materials was performed in order to obtain the area fraction of the phases of pearlite and sulfide inclusions. A mechanical characterization of the materials was also performed, consisting in a set of static (hardness and tension tests) and dynamic (Split Hopkinson Pressure Bar Test) tests at two different strain rates, with the objective of observing the deformation behavior of the sulfide inclusions at low and high strain rates, respectively. The behavior of the sulfide inclusions was observed to be brittle under low strain rates. On the other hand, under high strain rates, a plastic deformation behavior was observed with inclusions participating in the plastic flow of the metal matrix. The MnS inclusions volume fraction influences on both static and dynamic behavior of the steels studied.*

Keywords*: Steel, MnS inclusion, Hardness, Tension test, Hardness test, Split Hopkinson Pressure Bar.*

1. INTRODUCTION

The mechanical properties can be described as the relationship between the stress and the resistance of the material to deformation and fracture (ASM Metals Handbook, 1990). Hence, the design, use and manufacturing of a device are performed based on the mechanical properties of the material. There are constitutive equations established by Johnson-Cook (Johnson and Cook, 1985), Zerilli-Armstrong (Meyers, 1994; Sasso *et al.* (2008)), Cowper-Simonds (Jones, 1997) that take into account the strain rate since the response of the material to stress is significant different at high rates. Therefore, there are several tests to measure the mechanical properties, wherein the loading and the strain rates are different (ASM Metals Handbook, 1990).

The microstructure of the material (inclusions, precipitates, grain size and phases distribution, among others) also strongly influences the mechanical properties. Literature (ASM Metals Handbook, 1990; Dieter, 1991; Meyers, 1999) presents several examples of the effect of heat treatments on the mechanical properties obtained during tensile test. The presence of non-metallic inclusions usually has deleterious effects in steels' mechanical properties (Kiessling, 1978; Luo *et al.* (2001)). However, inclusions, such as: MnS, improve the machinability of steels since their presence propitiates the chip broken (Kiessling, 1978; Shaw, 2005). The inclusions in steels can show a brittle or plastic behavior depending on the strain rate as well as the temperature (Kiessling, 1978; Jiang *et al.* (1996)). Their morphology, distribution and aspect ratio are also important to evaluate the mechanical behavior of the steel (Antretter and Fischer, 1996, Nygards and Gudmundson, 2002; Vignal *et al.* (2003); Correa *et. al.* (2007a); Correa *et. al.* (2007b)). Models were proposed in the literature (Antretter and Fischer, 1996; Nygards and Gudmundson, 2002; Vignal *et al.* (2003)) to evaluate the effect of inclusions as stress-concentrating elements. However, the numerical modeling of the mechanical behavior of the steels is difficult since during the manufacturing process the strain, the strain rate and the microstructure are not homogeneous (Correa *et. al.* (2007a); Correa *et. al.*,(2007b)).

The main motivation of this work was to obtain data to evaluate the effect of inclusions on the mechanical behavior of steel at low and high strain rates, and also characterize the MnS inclusions, to simulate the machinability of the ABNT 1045 steels by means finite element method. Therefore, this work deals with the influence of sulfur on the mechanical properties, obtained through static and dynamic tests, of two different steels with chemical compositions within the ranges specified for AISI 1045, but with different sulfur contents. Hardness and tensile tests (quasi-static conditions) and Hopkinson bar tests (compressive dynamic conditions) were carried out to compare and discuss the behavior of the steels at different strain rates.

2. MATERIALS AND METHODS

2.1 Materials

The materials studied in this work were two different steels with chemical compositions within the ranges specified for AISI 1045. However, one of the steels presented slight higher sulfur content. The steel named as 1045 had 0.03 wt%S and the steel named as 1145 had 0.06wt%S. The specimens used in the tests were obtained from hot-rolled bars of 50mm in diameter. Table 1 shows the nominal chemical composition of the steels studied.

Table 1. Nominal chemical composition of the steels studied, wt% (ASM Metals Handbook, 1990).

Steel	%C	%Si	%Mn	%P	%S	%Cr
1045	0.43-0.50	0.15-0.35	0.60-0.90	Max 0.04	**0.03**	0.10-0.20
1145	0.42-0.49	0.15-0.35	0.70-1.00	Max 0.04	**0.06**	0.10-0.20

2.2 Microstructural characterization

The microstructures were observed by means of optical microscopy (OM) Olympus BX60M. The metallographic sample preparation for OM observations consisted of grinding down to 600-grit paper, followed by 1 μm diamond polishing. After polished, some of the samples were etched for a few seconds in Nital 3% for general microscopical examinations. The observation and quantitative metallography of inclusions were conducted in the samples before the etching. The quantitative metallography was carried out by means the software Leica Qwin, and 50 fields were analyzed.

The samples were also observed by means of scanning electron microscopy (SEM) Philips XL-30 and LEO 440e, mainly to observe the specimens after static and dynamic tests.

2.3 Mechanical characterization

2.3.1 Hardness

Hardness was measured in the longitudinal and transverse sections of the samples, using a Struers hardness tester (load of 300 N).

2.3.2 Tensile tests

The tensile tests were carried out to determine the yield, strength and elongation of the steels. The sample dimensions and geometry are showed in Fig.1a, following the ASTM 8M standard. All tensile tests were performed in an Instron machine model 3369 with load capacity of 50kN. The tensile test procedure is a standard one whereby the specimens are fixed in the machine jaws (see Fig. 1b). The imposed displacement rate of the jaws during the quasi-static experiments was 1.0mm/min. The load is measured by the calibrated machine load cell and the displacements by clip gauges with length of 50mm, fixed symmetrically to the center of the specimens. Three tensile tests were carried out for each steel (1045 and 1145 specimens).

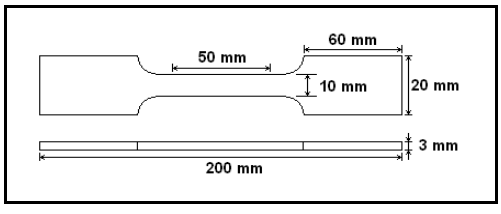

(a)

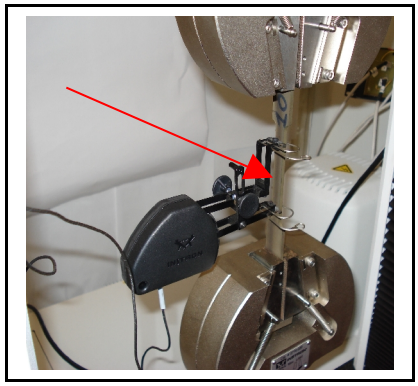

(b)

Figure 1. (a) Tensile tests specimens and (b) tensile specimen set up and the experimental apparatus. The clip gauge is attached in the specimens (red arrow).

2.3.3 Hopkinson bar compression tests

Samples were taken from the longitudinal and transverse sections of the rolled bars (Fig. 2a). Figure 2b shows the geometry and the dimensions of the specimens for the Hopkinson bar tests. The experimental procedure for dynamic material characterisation was based on the Split Hopkinson pressure bar (SHPB), which is also shown in Fig. 2c and Fig. 2d.

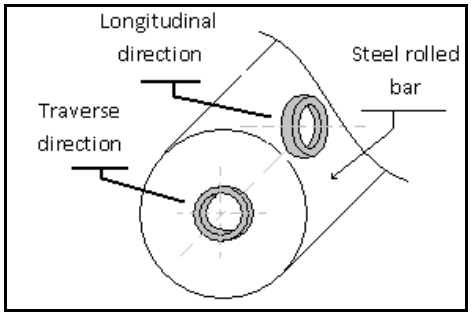

(a)

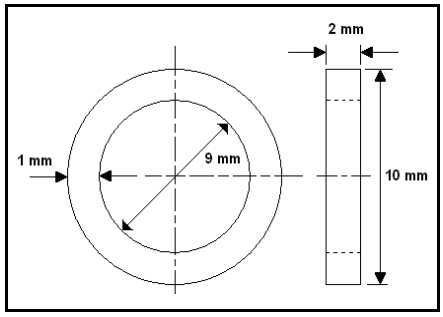

(b)

(c)

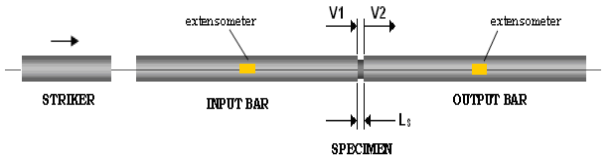

(d)

Figure 2. (a) Schematic illustration of region of the bar the specimens were taken from. (b) Geometry and dimensions of the specimens. (c) Hopkinson bar and (d) its schematic apparatus.

The Split-Hopkinson pressure bar experiment is idealized as a test to obtain the response of a material when subjected to large strain rates, in order of 10^2 to 10^4 s^{-1}. The test, as shown in the schematic part of Fig. 2d, consists of two long bars (called input and output bars) and a striker bar, all designed to remain elastic throughout test. Between input and output bars is positioned the specimen. The striker bar then is fired against one end of the input bar, and the collision produces a compressive pulse that propagates along it. The compressive pulse travels at a speed proportional to square root of elastic modulus divided by density of the steel bar. When the compressive pulse reaches interface input bar-specimen, part of the pulse is reflected and the other part is transmitted to specimen as a compressive pulse. In specimen, the compressive pulse meets another interface with output bar, and again a phenomenon of reflection with partial transmission of pulse occurs. In each reflection at an interface, the pulse changes phase from compression to tension or vice versa. Although several reverberations of the loading wave occur within the same test, the model used in this work refers to the first reflection of stress pulse.

Resistance strain gages are placed on the input and output bars for measuring the magnitude of the initial incident pulse in the input bar, the reflected pulse from the input bar-specimen interface and the transmitted pulse through the specimen to the output bar. The strain gages are located on bars in regions where incident and reflected pulses do not overlap, and the signals are measured by using high speed acquisition cards and computers. Based on assumptions such as the bars remain elastic throughout the test; no wave attenuation or dispersion occurs; the specimen remains in equilibrium throughout the test, one can relate the input and output bar signals with stress (σ_S, Eq. (1)), strain (ε_S, Eq. (2)) and strain rate ($\dot{\varepsilon}_S$, Eq. (3)), in the specimen,

$$\sigma_S = E_b \frac{A_b}{A_S} \varepsilon_T \tag{1}$$

$$\varepsilon_S = -2 \frac{C_0}{L_S} \int_0^t \varepsilon_R dt \tag{2}$$

$$\dot{\varepsilon}_S = -2 \frac{C_0}{L_S} \varepsilon_R \tag{3}$$

where $C_0 = \sqrt{E_b / \rho_b}$ is the elastic wave propagation velocity; ρ_b, A_b and E_b are, respectively, density, area and Young Modulus of the bars; A_s and L_s are, respectively, the cross section area and the length of the specimen. The reflected strain $\varepsilon_R(t)$ and transmitted strain $\varepsilon_T(t)$ are measured by the strain gages through, respectively, reflected tension pulse and transmitted compression pulse. The tests were carried out three times for each steel.

3. RESULTS AND DISCUSSION

3.1 Microstructural characterization

The microstructure of the longitudinal section is shown in Fig. 3, as the most representative of the 1045 steel bar since the inclusions are needle-shaped whilst Tab. 2 displays the results of quantitative metallography.

The microstructure of the longitudinal section of the 1145 steel bar is shown in Fig. 4 and Tab. 3 displays the results of quantitative metallography. Table 4 shows the average values of length, width and the aspect ratio (length/width) of the needle-shaped MnS inclusions of the steels studied.

The results show that the main differences between the 1045 and the 1145 steels are the volume fractions of the MnS inclusions and the average width of the inclusions. The grain size and the volume fraction of pearlite can be considered the same.

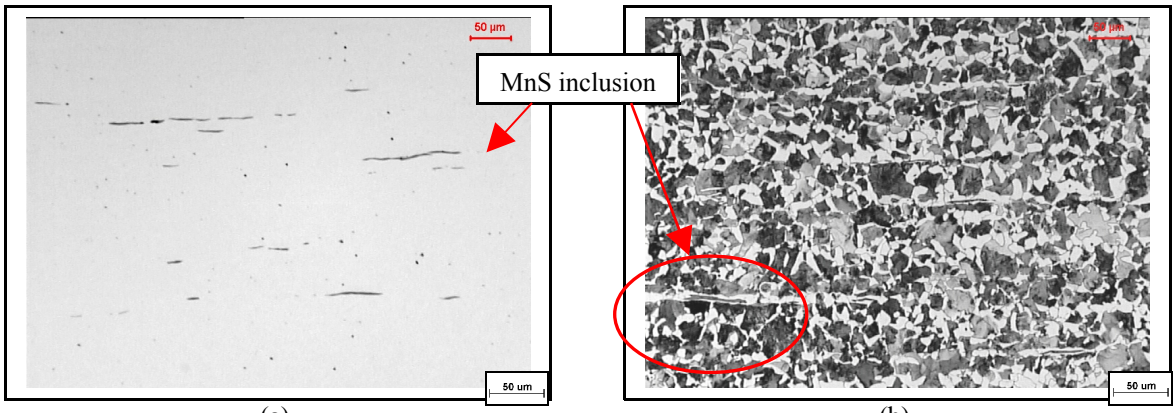

(a) (b)

Figure 3. (a) Black lines are the MnS inclusions in the steel matrix (no etching). (b) The MnS inclusions can be observed inside the ferritic regions, the gray regions are pearlite, which can be observed after the etching with Nital 3%. Material: 1045 steel.

Table 2. Quantitative metallography, 1045 steel: volume fraction of pearlite (%), steel grain size (µm) and volume fraction of MnS inclusions (%), longitudinal section of the rolled bar.

Vol fraction of pearlite (%)	69±3
steel grain size (µm)	26.4±2.2
Vol fraction of MnS inclusions (%)	0.20 ± 0.01

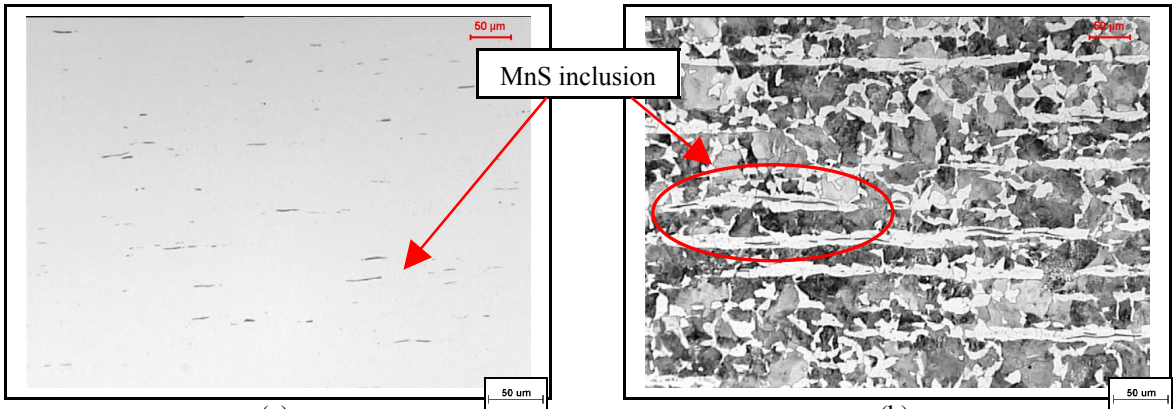

Figura 4. (a) Black lines are the MnS inclusions in the steel matrix (no etching). (b) The MnS inclusions can be observed inside the ferritic regions, the gray regions are pearlite, which can be observed after the etching with Nital 3%. Material. 1145 steel.

Table 3. Quantitative metallography, 1145 steel: volume fraction of pearlite (%), steel grain size (µm) and volume fraction of MnS inclusions (%), longitudinal section of the rolled bar.

Vol fraction of pearlite (%)	71±3
steel grain size (µm)	26.5±2.5
Vol fraction of MnS inclusions (%)	0.40±0.18

Table 4. Average values of length (L), width (W) and the aspect ratio (L/W) of the MnS inclusions in the steels studied.

Steel	**L (µm)**	**W**	**L/W**
1045	22.4±13.8	1.9±1.0	15.0±12.9
1145	22.0±15.6	2.2±1.1	10.3±6.1

3.2 Mechanical characterization

3.2.1 Hardness

The hardness of the steels studied is shown in Tab. 5. The 1145 steel is harder than the 1045 though, both present homogenous hardness in the transverse and longitudinal section of the bar.

Table 5. Hardness (HV 30) of the 1045 and 1145 steel.

HV - steel	1045	1145
Transverse section	210±5	243±1
Longitudinal section	214±2	234±4

3.2.2 Tensile tests

The tensile tests were conducted at $3x10^{-3}$ s^{-1} (strain rate). Hence, the tests can be considered quasi-static for these materials. Figure 5 shows the stress-strain curves and Tab. 6 shows the average mechanical properties and standard deviation obtained for the 1045 and 1145 steel. In Fig. 5b only two curves are showed for 1145 steel, due to a problem in the acquisition throughout one of the tensile tests, though they are representative (see Fig. 6) since the specimens showed similar behavior.

The 1145 steel shows higher yield and strength, as previous results of hardness, and lower elongation than 1045 steel. The decrease in the ductility can be related to the higher volume fraction of MnS inclusions. The 1045 steel also presented a discontinuous yielding, which was not observed in the 1045 steel.

Figure 6 shows the specimens tested whilst Fig. 7 shows the fracture surfaces of each steel after the tensile tests. A detachment occurred in the interface between the inclusions and the steel matrix during the steel deformation. However, the MnS inclusions fracture occurred without deformation as can be observed in Fig. 7. This behavior can be related to the lower ductility of the 1145 steel, which presents higher volume fraction of inclusions.

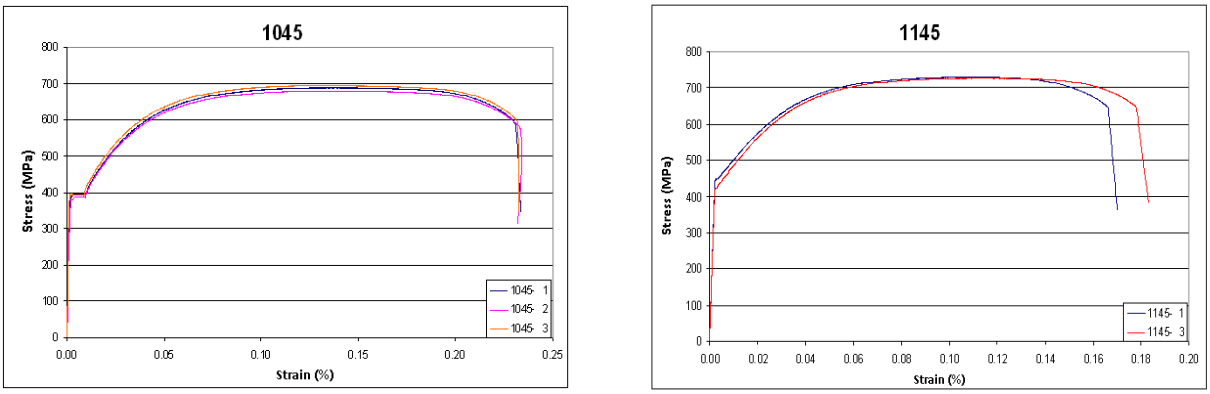

(a) (b)

Figure 5. Stress-strain curves. (a) 1045 steel. (b) 1145 steel.

Table 6. Mechanical properties of 1045 and 1145 steel – Tensile tests.

Mechanical properties	**1045**	**1145**
Young modulus (E)	236 ± 26 GPa	220 ± 6 GPa
Yield (S_y)	384 ± 7 MPa	431 ± 13 MPa
Strength (S_u)	687 ± 7 MPa	730 ± 2 MPa
Elastic strain (ε_y)	0.2 %	0.2 %
Elongation (ε_u)	13.4 %	11.0 %
Total strain (ε_{max})	23.3 %	17.7%

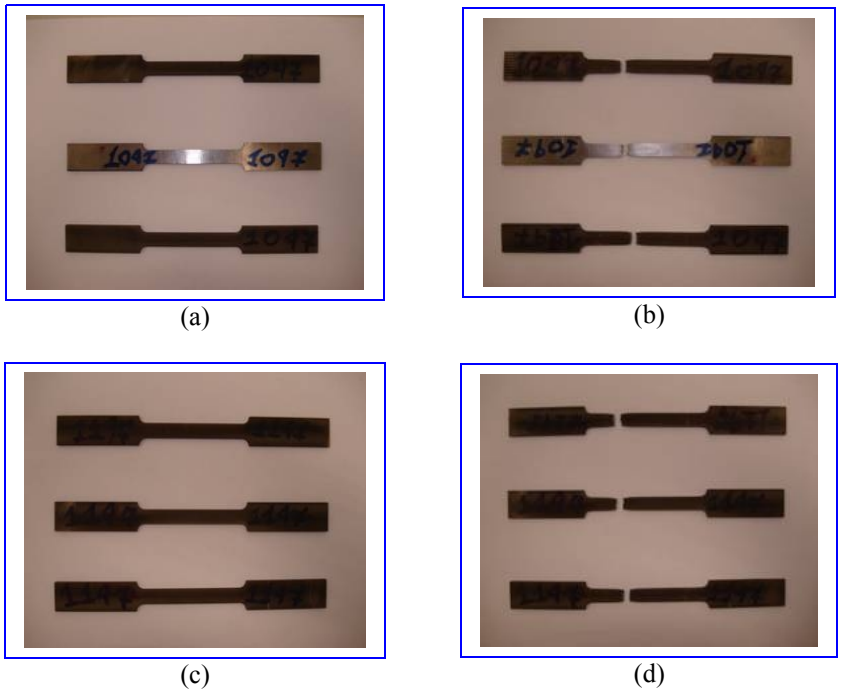

(a) (b)

(c) (d)

Figure 6. Specimens (a) and (c) before and (b) and (d) after tensile tests. (a) and (b) 1045 steel and (c) and (d) 1145 steel.

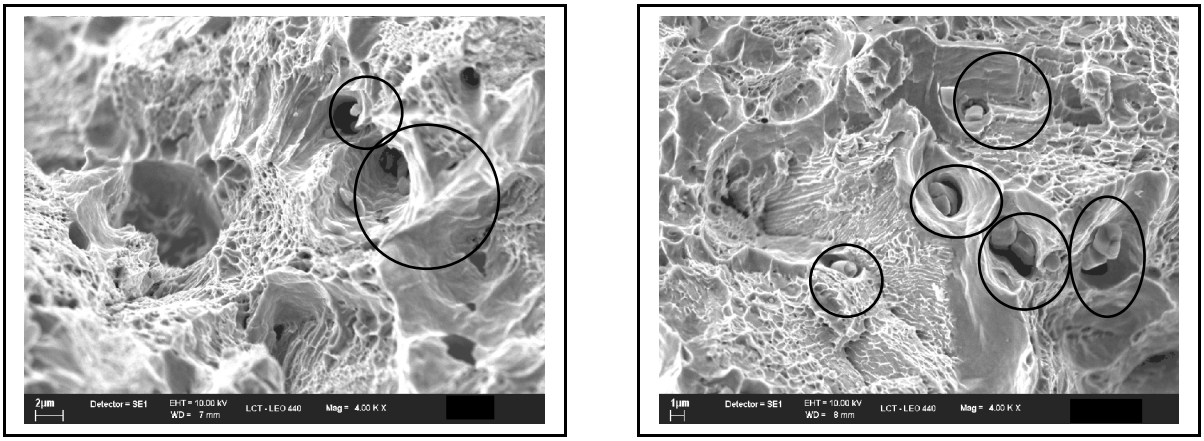

(a) (b)

Figure 7. Fracture surface after tensile test (a) 1045 and (b) ABNT 1145. The circles indicate the MnS inclusions regions. SEM, secondary electrons.

3.2.3 Hopkinson bar tests

The Hopkinson bar tests (SHPB) were carried out in the samples taken from the longitudinal section of the rolled bars of 1045 and 1145 steels (see Fig. 2a). SHPB tests were also carried out in the samples taken from transverse section of the 1145 steel bar (see Fig. 2a). Two different strain rates were utilized (about 1000 s^{-1} and 3000 s^{-1}). Figure 8 displays the results of SHPB tests (stress-strain curves) for 1045 steel (longitudinal section) whilst Fig. 9 shows the results of stress-stress curves for the 1145 steel (longitudinal and traverse sections). Tables 7 and 8 displays the average results and standard deviation for the different strain rates used in the SHPB tests. The higher the strain rate, the higher the yield and the strength. The opposite occurred with the ductility of the steels studied.

The 1145 steel showed slight high mechanical properties than the 1045 steel, as observed in the previous results of hardness and tensile tests. The other important result was obtained from the longitudinal and transverse sections comparison. The transverse section presented higher ductility than the longitudinal one. This result shows the importance of microstructural features even at high strain rates. It is worth mentioning that the mechanical properties obtained at high strain rates were about 10 times greater than that obtained in tensile tests. Although, the strain rate has a huge effect on the mechanical properties, the microstructurals features have influenced on the mechanical properties and they have to be considered characterize the material and model the mechanical behavior.

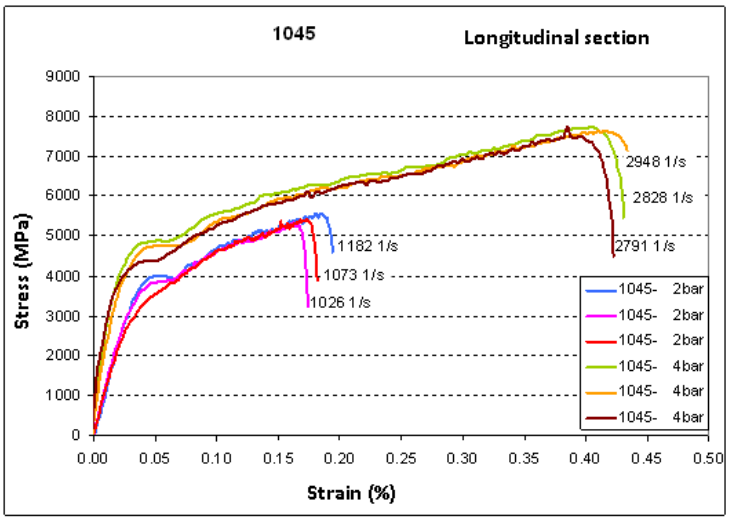

Figure 8. Stress-strain curves obtained from SHPB tests. 2 bar of pressure in the sticker led to a 1000 s^{-1} strain rate and 4 bar led to 3000 s^{-1}. 1045 steel, longitudinal section of the steel bar(Fig. 2a).

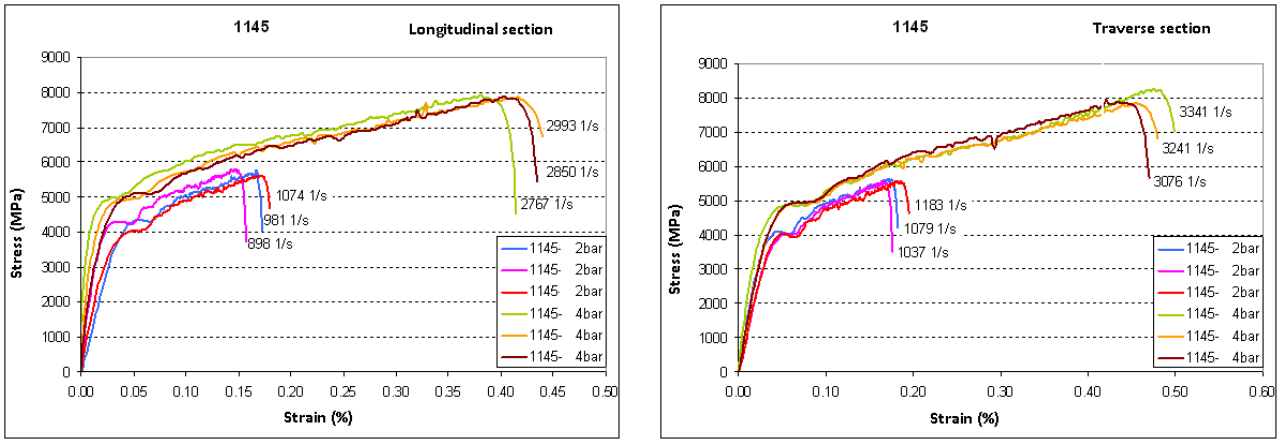

(a) (b)

Figure 9. Stress-strain curves obtained from SHPB tests. 2 bar of pressure in the sticker led to a 1000 s^{-1} strain rate and 4 bar led to 3000 s^{-1}. 1145 steel, (a) longitudinal and (b) transverse sections (Fig. 2a).

Table 7. Mechanical properties obtained from the stress-strain curves of SHPB tests carried out at 1000 s^{-1} (strain rate).

Mechanical properties	**1045 (longitudinal)**	**1145 (longitudinal)**	**1145 (traverse)**
Strain rate	1093±80 (s^{-1})	984±88 (s^{-1})	1100±75 (s^{-1})
Yield (S_y)	3881± 66 MPa	4203 ± 13 MPa	4037± 9 MPa
Strength (S_u)	5426 ± 108 MPa	5741 ± 97 MPa	5574 ± 37 MPa
Elastic strain (ε_y)	0.61 %	0.53 %	0.55 %
Elongation (ε_u)	17.2 %	15.2 %	17.2 %
Total strain (ε_{max})	18.4 %	17.0 %	18.5 %

Table 8. Mechanical properties obtained from the stress-strain curves of SHPB tests carried out at 3000 s^{-1} (strain rate).

Mechanical properties	**1045 (longitudinal)**	**1145 (longitudinal)**	**1145 (traverse)**
Strain rate	2855±82 (s^{-1})	2870±114 (s^{-1})	3219±134 (s^{-1})
Yield (S_y)	4665±247 MPa	5010± 81 MPa	4902±59 MPa
Strength (S_u)	7657 ± 102 MPa	7885±20 MPa	8019± 217 MPa
Elastic strain (ε_y)	0.50 %	0.47 %	0.71 %
Elongation (ε_u)	42.0%	40.0 %	42.0 %
Total strain (ε_{max})	43.4 %	43.2 %	48.7 %

Figures 10 and 11 show the microstructure of the 1145 steel after the SHPB tests carried out at 3000 s^{-1} (strain rate) where the deformation of the steel matrix as well as the MnS inclusions can be observed. Crack formation occurred in the MnS inclusion. However, the cracks were mainly observed in the interface between the steel and the MnS inclusions (Fig. 11b). Therefore, at high strain rates the MnS inclusions show different behavior. They deform, contrary to that observed after tensile tests. This result is very important to discuss and propose a model at high strain rates, such as in machining. The deformation behavior of the MnS inclusions at high strain rates is very different from the one found at low strain rates. Probably, a local increase in the temperature occurred, similar to the adiabatic shear in machining (Shaw, 2005), leading to the inclusion deformation at high strains.

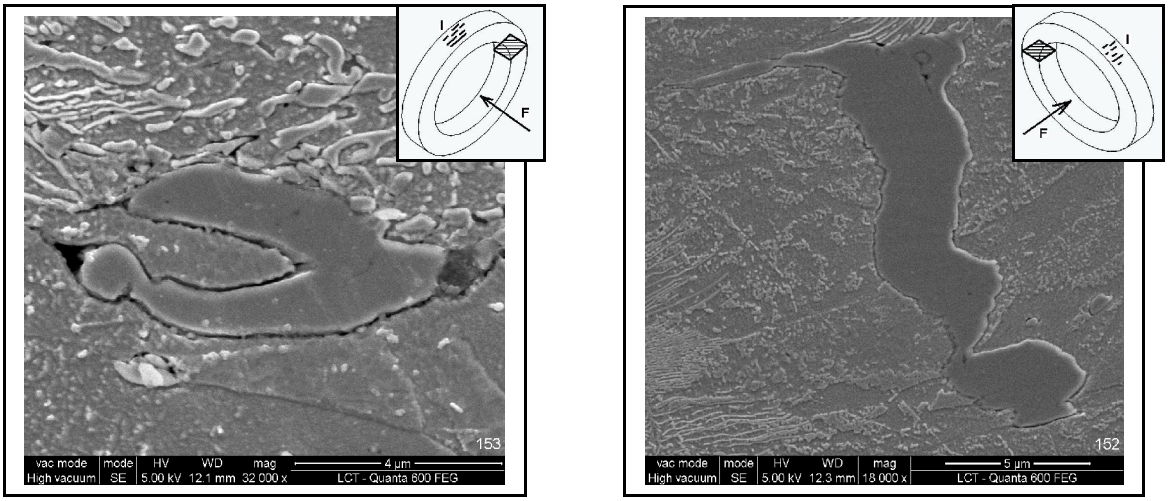

(a) (b)

Figure 10. Micrographs of the 1145 steel after SHPB tests with different magnitudes. (a) longitudinal section and (b) traverse section of the 1145 steel bar. SEM, secondary electrons.

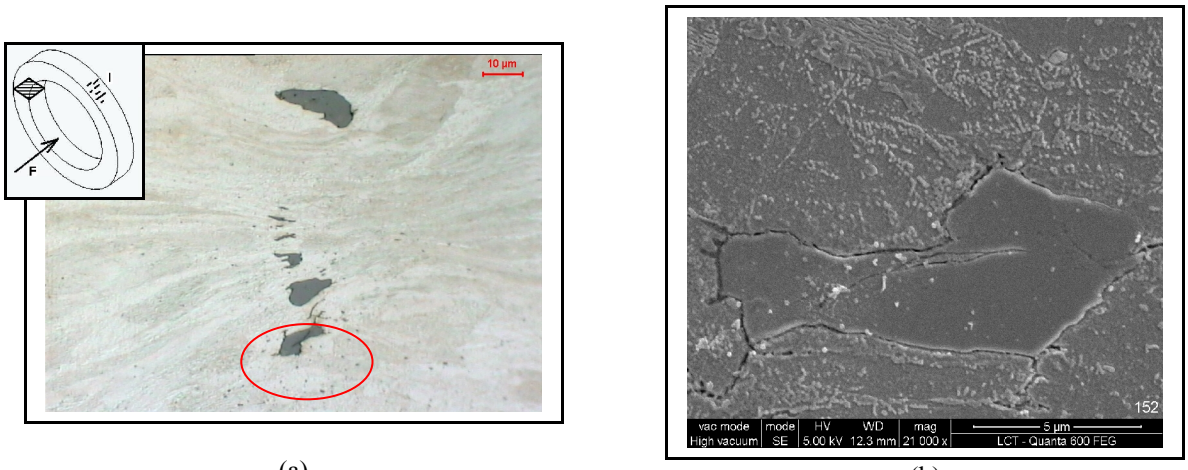

(a) (b)

Figure 11. Micrographs of the 1145 steel after SHPB tests. Transverse specimen of the 1145 steel bar. (a) Optical microscopy, detail of the region circled is shown in (b), SEM, secondary electrons.

4. CONCLUSIONS

The microstructural and mechanical characterization of two different steels with chemical compositions within the ranges specified for AISI 1045, but with different sulfur contents were carried out. The influence of sulfur volume fraction on the mechanical properties was observed through hardness and tensile tests (quasi-static conditions) and Hopkinson bar tests (dynamic conditions). The results of this work allow the following conclusions:

1. The strain rate has strong effect on the mechanical properties of the studied steel. The strength obtained at high strain rates was about 10 times greater than that obtained in tensile tests. This point is relevant when discussing and a deformation and fracture model at high strain rates, such as in machining.
2. The 1145 steel, which has the higher sulfur content, presents the higher mechanical properties and the lower ductility, hence the volume fraction of the MnS influenced the mechanical behavior at high and low strain rates.
3. The MnS inclusions deformed at the highest strain rates, contrary to that observed after tensile tests. Probably, there was a local increase in the temperature due the high strain rate, similar to adiabatic shear.
4. The influence of microstructure is also observed in the results of the transverse and longitudinal section of the steel bars. The orientation of the inclusion, in relation to the loading, affects the ductility of the material. The transverse section presented the highest ductility.

5. ACKNOWLEDGEMENTS

The author would like to thank CNPq (National Counsel of Technological and Scientific Development) of Brazilian Government for financial support, FAPESP (Fundação de Amparo à Pesquisa , São Paulo), CAPES (Coordenação de Aperfeiçoamento de Pessoal de Nível Superior) and FINEP – Aços Villares S.A. (Ação Transversal MCT/FINEP. Process number 01.04.087.00).

6. REFERENCES

Antretter, T. and Fischer, F.D., 1996, " The Stress State Around Two Spatially Arranged Ellipsoidal Inclusions - A Case Study for High-Speed Tool Steel", Computational Materials Science, Vol. 7, pp. 247-252.

"ASM Metals Handbook - Properties and Selection Irons, Steels, and High Performance Alloys", 1990, ASM. USA:, v. 1. 1618p.

Correa, P.A., Gonzalez, D.F., Souza, R.M., Machado, I.F. and Sinatora, A., 2007a,"Estudio de da Maquinabilidad de Aceros Medio Carbono por Medio del Método de los Elementos Finitos", Procedings of the CIBIM 2007. 8º Congreso Iberoamericano de Ingenieria Mecanica, Cusco, Perú.

Correa, P.A, González, D.F, Souza, R.M and Machado, I.F., 2007b," Stress analysis of the machining process through finite element method (FEM): Effect of a single MnS inclusion", Proceedings of the COBEM 2007. 19th International Congress of Mechanical Engineering, Brasilia, Brazil.

Dieter, G.E., 1981, "Metalurgia Mecânica", Editora Guanabara Koogan S.A, Rio de Janeiro, Brazil, 653 p.

Jiang L., Cui K., Hänninen H., 1996, "Effects of the Composition, Shape Factor and Area Fraction of Sulfide Inclusions on the Machinability of Re-Sulfurized Free-Machining Steel", Journal of Materials Processing Technology, Vol. 58, pp. 160-165

Johnson, G.R. and Cook, W.H., 1985," Fracture Characteristics of Three Metals Subjected to Various Strains, Strain Rates, Temperatures and Pressures", Engineering Fracture Mechanics, Vol. 21, pp. 31-48.

Kiessling, R. and Lange, N., 1978," Non-Metallic Inclusions in Steel". The Metals Society, London, UK, 258p.

Luo, C and Stalhberg, U., 2001, " Deformation of inclusions during hot rolling of steels", Journal of Materials Processing Technology, Vol.114, pp. 87-97.

Meyers, M.A and Chawla, K.K., 1999, "Mechanical Behavior of Materials", Prentice-Hall, New Jersey, USA, 680p.

Meyers, M.A., 1994, " Dynamic Behavior of Materials" John Wiley & Sons Inc., New York, USA, 668p.

Jones, N., 1997, "Structural Impact", Cambridge University Press, London, UK, 575p.

Nygards, M. and Gudmundson, P., 2002, " Micromechanical Modeling of Ferritic/Pearlitic Steels", Materials Science and Engineering, Vol. A325, pp. 435-443.

Sasso, M., Newaz, G. and Amodio, D., 2008, " Material Characterization at High Strain Rate by Hopkinson Bar Tests and Finite Element Optimization", Materials Science and Engineering, Vol. 487, pp. 289-300.

Shaw, M.C., 2005, "Metal Cutting Principles" Oxford University Press, New York, USA, 651 p.

Vignal, V., Oltra, R. and Josse, C., 2003, " Local Analysis of the Mechanical Behaviour of Inclusions-Containing Stainless Steels Under Straining Conditions", Scripta Materialia, Vol. 49, pp. 779-784.

7. RESPONSIBILITY NOTICE

The authors are the only responsible for the printed material included in this paper.